PHILOSOPHICAL MAGAZINE, 1–11 SEPTEMBER 2004
VOL. 84, NOS. 25–26, 2777–2792

In-situ observation of dislocation motion in icosahedral Al–Pd–Mn quasicrystals

F. MOMPIOU, D. CAILLARD†

Centre d'Elaboration des Matériaux et d'Etudes Structurales, BP4347, F-31055 Toulouse Cedex, France

and M. FEUERBACHER

Forschungszentrum Jülich GmbH, D-52425 Jülich, Germany

[*Received 31 March 2003 and accepted in revised form 8 September 2003*]

ABSTRACT

Dislocation motion in icosahedral Al–Pd–Mn quasicrystals has been observed *in situ* in a transmission electron microscope between 700 and 750°C. Contrast analyses show that it takes place by pure climb in twofold, threefold and fivefold planes. Moving dislocations exhibit polygonal shapes with edges parallel to two-fold directions, in agreement with a difficult jog-pair nucleation. Dislocation multiplication, annihilation and local pinning are described and discussed, as well as the role of the phason faults trailed in the wake of dislocations, at the lowest investigated temperatures.

§ 1. INTRODUCTION

Plastic deformation of icosahedral Al–Pd–Mn quasicrystals takes place by dislocation motion and multiplication as in crystals (Wollgarten *et al.* 1993). Dislocations in quasiperiodic structures can be generated by means of a Volterra process. However, two generally different procedures can be followed:

(i) As in any solid, a Volterra process in the three-dimensional physical space, that is a cut along an arbitrary direction and distance followed by an adequate displacement of the two halves of the structure, can be performed. Since the icosahedral structure lacks periodicity, this procedure necessarily leads to the introduction of a planar fault in the cut plane, and the terminating dislocations are imperfect. As in crystals, the energy of the planar fault possesses local minima for specific displacement vectors $\mathbf{b}_{//}$, which will be discussed later. The corresponding planar faults and dislocations are favoured.

(ii) The Volterra process can be performed in the six-dimensional hypercubic lattice from which the icosahedral structure is deduced by cut and projection into the three-dimensional physical space (for example Cahn *et al.* (1986)). If the two hypercrystal halves of the cut are displaced by a translationally invariant Burgers vector $\mathbf{B}$ of the six-dimensional lattice, they can

† Author for correspondence. Email: caillard@cemes.fr.

Philosophical Magazine ISSN 1478–6435 print/ISSN 1478–6443 online © 2004 Taylor & Francis Ltd
http://www.tandf.co.uk/journals
DOI: 10.1080/14786430410001671494

be perfectly sealed and a perfect dislocation is obtained. After cut and projection into physical space, the dislocation consequently remains perfect and the structure around the dislocation line is only locally distorted with respect to the original six-dimensional lattice. Accordingly, the Burgers vector of the so-constructed dislocation is described by six components, three of which describe the physical-space elastic field ($\mathbf{b}_{//}$) and the remaining three describe their 'phason-displacement' component ($\mathbf{b}_{\perp}$) (Yang *et al.* 1998).

The phason-displacement field of a perfect dislocation constructed after procedure (ii) is physically realized by a cloud of chemical and structural point defects locally surrounding the dislocation line. On the other hand, the planar fault created performing process (i) consists of a planar agglomeration of phasons, that is chemical and structural point defects allowing for the continuation of the two structure halves. The Burgers vector of the terminating imperfect dislocation can, as for the case of the perfect dislocation, be described by a physical-space Burgers vector component $\mathbf{b}_{//}$. It can be considered a projection of a six-dimensional Burgers vector **B**. In physical space, a transition from one situation to the other, that is from an imperfect to a perfect dislocation in physical space possessing the same Burgers vector component $\mathbf{b}_{//}$ can be considered, taking place by dissolution of the planar fault connected to the imperfect dislocation and local rearrangement of an appropriate density of phason defects around the dislocation line. Conversely, the planar faults can be considered a condensation of individual phasons. For this reason, the planar faults have been termed 'phason faults' or, occasionally, 'phason walls', and their dissolution is called 'phason dispersion' or 'retiling'. This transition process has been observed experimentally by Feuerbacher *et al.* (2004).

Both types of dislocation have been observed in transmission electron microscopy (TEM). Imperfect dislocations terminating phason faults are found at low temperatures whereas perfect dislocations are found at high temperatures (Rosenfeld *et al.* 1995, Caillard *et al.* 1999, 2000, Caillard 2000, Mompiou *et al.* 2003). This is a consequence of the strong thermal activation of the phason diffusion process (Feuerbacher *et al.* 2004).

The contrast of dislocations and phason faults in TEM obeys the classical rules established for defects in crystals, but the phase shifts must be computed in six-dimensional space. This allows the determination of dislocation Burgers vectors and planar-fault displacement vectors (Wollgarten *et al.* 1991, Mompiou *et al.* 2003).

In previous work, dislocations have been analysed in deformed specimens, but as the form an isotropic 3D network their corresponding planes of motion could not be determined (Rosenfeld *et al.* 1995). Conversely, *in-situ* tensile tests have shown dislocations moving in various planes, but the corresponding Burgers vectors could not be determined (Wollgarten *et al.* 1995, Messerschmidt *et al.* 1999). Partly because of this indetermination, dislocations have been assumed to move by gliding, in the planes containing their line direction and their Burgers vector component in physical space. Several glide mechanisms have been subsequently proposed and simulated to account for their strongly thermally activated motion (Feuerbacher *et al.* 1997, Schaaf *et al.* 2000, Takeuchi *et al.* 2002).

The first evidence of dislocation climb in icosahedral Al–Pd–Mn has been obtained in as-grown samples (Caillard *et al.* 1999, 2000, 2002a,b, 2003). Further observations confirmed that climb is a very active mechanism of dislocation motion in this material (Mompiou *et al.* 2003) and climb is now considered as a possible deformation mechanism of Al–Pd–Mn by other workers (Messerschmid and Bartsch 2003). In the present publication we report the first *in-situ* experiments for which Burgers vectors and planes of motion have been determined simultaneously, and for which pure climb dislocation motion could be unambiguously demonstrated.

§ 2. Experimental details

In the present study, single-quasicrystal icosahedral Al–Pd–Mn samples, produced by means of the Czochralski technique, were investigated. The single quasicrystals were grown by Y. Calvayrac (Vitry, France) and M. Feuerbacher (Jülich, Germany). The growth directions were chosen parallel to fivefold quasi-lattice directions, and the compositions of the final quasicrystals were about 70.1 at.% Al–20.4 at.% Pd–9.5 at.% Mn. Specimens for TEM investigation were prepared by subsequent grinding, polishing and ion milling or wet-chemical thinning. The sample normals were chosen parallel to the fivefold [1/0, 0/1, 0/0] growth direction and the twofold $[1/1, 0/1, \bar{1}/0]$ direction (indexing according to Cahn *et al.* (1986)). These samples will be referred to in the following as fivefold and twofold samples respectively.

In a first set of experiments, samples were heated in a JEOL 2010 HC transmission electron microscope operated at 200 kV. Special care has been devoted to the sample fixation in the holder to ensure good thermal contact with the furnace. Under these conditions, the temperature of the observed specimen area was checked to be equal to that of the furnace within $\pm 5^\circ$C. The experiments were performed at a sufficiently high temperature (above 700°C) to activate dislocation motion under thermal and internal stresses present in the foil. The planes of motion were deduced from their trace direction and apparent width as a function of the specimen tilt angle. For closer characterization, moving dislocations were frozen by rapid cooling to room temperature, and their Burgers vectors were determined by contrast analysis (Wollgarten *et al.* 1991, Mompiou *et al.* 2003). Diffraction patterns taken during and after heating unambiguously show that the icosahedral structure is preserved during the experiments.

In a second set of experiments, microsamples were strained along a twofold axis in a high-temperature straining holder. The experiments were carried out rapidly enough to avoid excessive sample degradation, and diffraction patterns were carefully analysed in order to ensure that no phase transitions have taken place during experiments.

Dislocations were imaged under two-beam conditions using diffraction vectors along fivefold and twofold physical-space directions. They are denoted $\mathbf{g}_{5i}$, $\mathbf{g}_{2i}$ and $\tau\mathbf{g}_{2i}$ respectively, where τ is the golden mean. They are projections of the corresponding six-dimensional diffraction vectors $\mathbf{G}$ and expressed in the coordinate system of the six-dimensional space (tables 1 and 2) (Cahn *et al.* 1986).

§ 3. Observations

3.1. *Dislocation motion in twofold planes*

Figure 1 shows a video-frame sequence of a dislocation moving in a twofold plane at 700°C in a fivefold specimen. The motion is viscous and the average velocity is 0.15 μm s^{-1}. It trails an externally bright fringe contrast which 12 s later has fully

Table 1. Contrast analysis of the dislocation in figure 9, with $\mathbf{B} = A_0[\bar{1}\,1\,1\,1\,1\,\bar{1}]$, $\mathbf{b}_{//} = a_0[\bar{2}/2, 2/0, 0/0]$ and $b_{//} = 0.563$ nm.

$\mathbf{g}_{//}$	**G**	**G·B**	Contrast
$\mathbf{g}_{2a} = 0/0, 0/0, \bar{2}/\bar{4}$	$0\bar{1}\bar{2}01\bar{2}$	0	Strong extinction (residual contrast)
$\tau\mathbf{g}_{2a} = 0/0, 0/0, \bar{4}/\bar{6}$	$0\bar{2}\bar{3}02\bar{3}$	0	Strong extinction (residual contrast)
$\mathbf{g}_{2b} = 1/2, \bar{1}/\bar{1}, \bar{2}/\bar{3}$	$00\bar{2}\bar{1}2\bar{1}$	0	Strong extinction
$\tau\mathbf{g}_{2b} = 2/3, \bar{1}/\bar{2}, \bar{3}/\bar{5}$	$00\bar{3}\bar{2}3\bar{2}$	0	Strong extinction
$\mathbf{g}_{2c} = 2/3, \bar{1}/\bar{2}, \bar{1}/\bar{1}$	$01\bar{1}\bar{2}20$	0	Strong extinction
$\tau\mathbf{g}_{2c} = 3/5, \bar{2}/\bar{3}, \bar{1}/\bar{2}$	$02\bar{2}\bar{3}30$	0	Strong extinction
$\mathbf{g}_{2d} = 1/1, 2/3, 1/2$	212100	2	Double contrast

Table 2. Contrast analysis of dislocations in figures 11 and 12, with $\mathbf{B} = A_0$ [000222], $\mathbf{b}_{//} = a_0[\bar{2}/2, \bar{2}/2, \bar{2}/2]$ and $b_{//} = 0.513$ nm.

$\mathbf{g}_{//}$	**G**	**G·B**	Contrast
$\mathbf{g}_{2a} = \bar{1}/\bar{2}, 1/1, \bar{2}/\bar{3}$	$0\bar{2}\bar{1}10\bar{2}$	−2	Double
$\tau\mathbf{g}_{2a} = \bar{2}/\bar{3}, 1/2, \bar{3}/\bar{5}$	$0\bar{3}\bar{2}20\bar{3}$	−2	Double
$\mathbf{g}_{2b} = 0/0, 0/0, \bar{2}/\bar{4}$	$0\bar{1}\bar{2}01\bar{2}$	−2	Double
$\tau\mathbf{g}_{2b} = 0/0, 0/0, \bar{4}/\bar{6}$	$0\bar{2}\bar{3}02\bar{3}$	−2	Double
$\mathbf{g}_{2c} = 1/2, \bar{1}/\bar{1}, \bar{2}/\bar{3}$	$00\bar{2}\bar{1}2\bar{1}$	0	Weak extinction
$\tau\mathbf{g}_{2c} = 2/3, \bar{1}/\bar{2}, \bar{3}/\bar{5}$	$00\bar{3}\bar{2}3\bar{2}$	−2	Double
$g_{2d} = 1/2, 1/1, \bar{2}/\bar{3}$	$10\bar{1}02\bar{2}$	0	Strong extinction
$\tau\mathbf{g}_{2d} = 2/3, 1/2, \bar{3}/\bar{5}$	$20\bar{2}03\bar{3}$	0	Strong extinction
$\mathbf{g}_{2e} = 2/3, \bar{1}/\bar{2}, \bar{1}/\bar{1}$	$01\bar{1}\bar{2}20$	0	Strong extinction
$\tau\mathbf{g}_{2e} = 3/5, \bar{2}/\bar{3}, \bar{1}/\bar{2}$	$02\bar{2}\bar{3}30$	0	Strong extinction
$\mathbf{g}_{5a} = 0/0, 1/2, \bar{2}/\bar{3}$	$1\bar{1}\bar{1}11\bar{2}$	0	Weak extinction

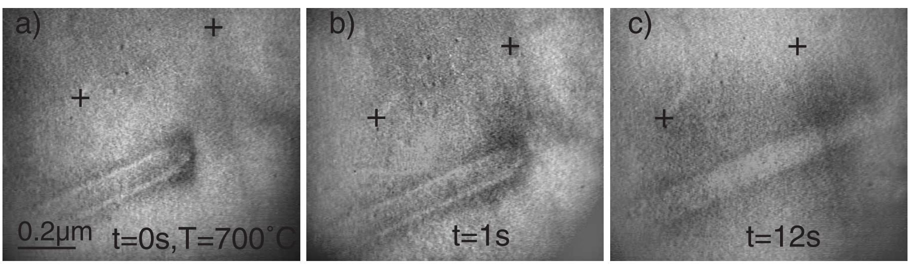

Figure 1. Dislocation motion in a twofold plane at 700°C. Note the fringe contrast behind the moving dislocation in (a) and (b), which has disappeared in (c). The crosses indicate fixed points in the sample.

disappeared (see figure 1 (c)). This fringe contrast is ascribed to a phason fault vanishing by phason dispersion.

Figure 2 shows a similar sequence in a twofold sample at a slightly higher temperature (720°C). The dislocation velocity is accordingly higher ($1.6\,\mu\mathrm{m\,s^{-1}}$), which explains the blurred appearance of the dislocations in the micrograph. It trails two straight dark traces at the sample surfaces, labelled t_1 and t_2, which do not evolve rapidly with time. A dark fringe is also visible between the traces, over the distance λ from the dislocation. It is interpreted as a phason fault which disappears

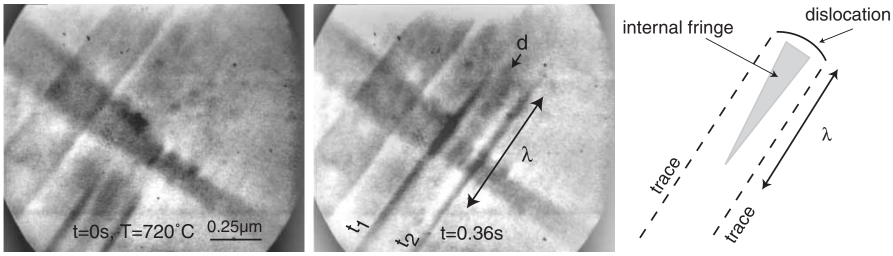

Figure 2. Dislocation motion in a twofold plane at 720°C. The dislocation d is blurred because of its high velocity. The traces at the sample surfaces are labelled t_1 and t_2.

within 0.4 s by phason dispersion. The more rapid dispersion at 720°C shows that this process is strongly thermally activated.

Figure 3 shows a dislocation multiplication process in a twofold sample. The dislocation moves in a twofold plane close to the sample plane (figure 3 (a)). During its movement it is pinned at an obstacle P (figure 3 (b)) and accordingly divided into two segments denoted 1 and 2. Because of independent and nonplanar motion of the two half-dislocations on each side of P, an open loop denoted 3 is formed (figure 3 (c)), which subsequently expands (figures 3 (c)–(e)). The open loop intersects one sample surface along the trace t in figure 3 (e). This multiplication process is similar to those already observed in magnesium deformed in prismatic slip (Couret and Caillard 1985). In the present material, however, dislocation motion probably takes place by pure climb, as will be shown in the following sections. Note that the dislocations exhibit straight segments parallel to twofold and pseudo-twofold directions labelled 2 and p2 respectively, in the schematic diagram on the right of the two dislocations in figure 3 (e).

Figure 4 shows a composed image of subsequent video frames at the grazing angle. The traces left behind by a dislocation labelled d moving in a twofold plane can be seen. The traces are clearly wavy, which shows that the motion is not perfectly planar, as already observed in previous post-mortem observations (Caillard *et al.* 1999, 2000).

3.2. *Dislocation motion in fivefold planes and Burgers vector analysis*

Figure 5 shows a dislocation in a twofold sample moving in a fivefold plane. The motion is as viscous as in twofold planes, but more planar, as illustrated by the grazing view in figure 6 (compare with figure 4). The velocities of the straight dislocation segments d_1 and d_2, parallel to twofold directions, are not constant. Between figures 5 (a) and (d), d_1 is faster than d_2, which leads to its shortening at the benefit of d_2. Subsequently, between figures 5 (e) and (i), d_2 is faster than d_1, which leads to a reversal of the length proportions.

In figure 7 (a), the same dislocation moving in the same plane as above has straight edges parallel to several twofold directions and one pseudo-twofold direction. The traces of these directions are shown in figure 7 (a) and are labelled 2 and p2 respectively. The segment parallel to the pseudo-twofold direction in the figure 7 (a) had rotated anticlockwise in figure 7 (b). It rotates further around an extrinsic pinning point P in figures 7 (b) and (c). A large 'macrojog' is then formed at the pinning point in figures 7 (d) and (e). When the dislocation escapes from the pinning point, it recovers its straight shape by fast lateral motion of the macrojog (figures 7 (f) and (g)). This sequence shows, firstly, that fivefold dislocations tend to align along

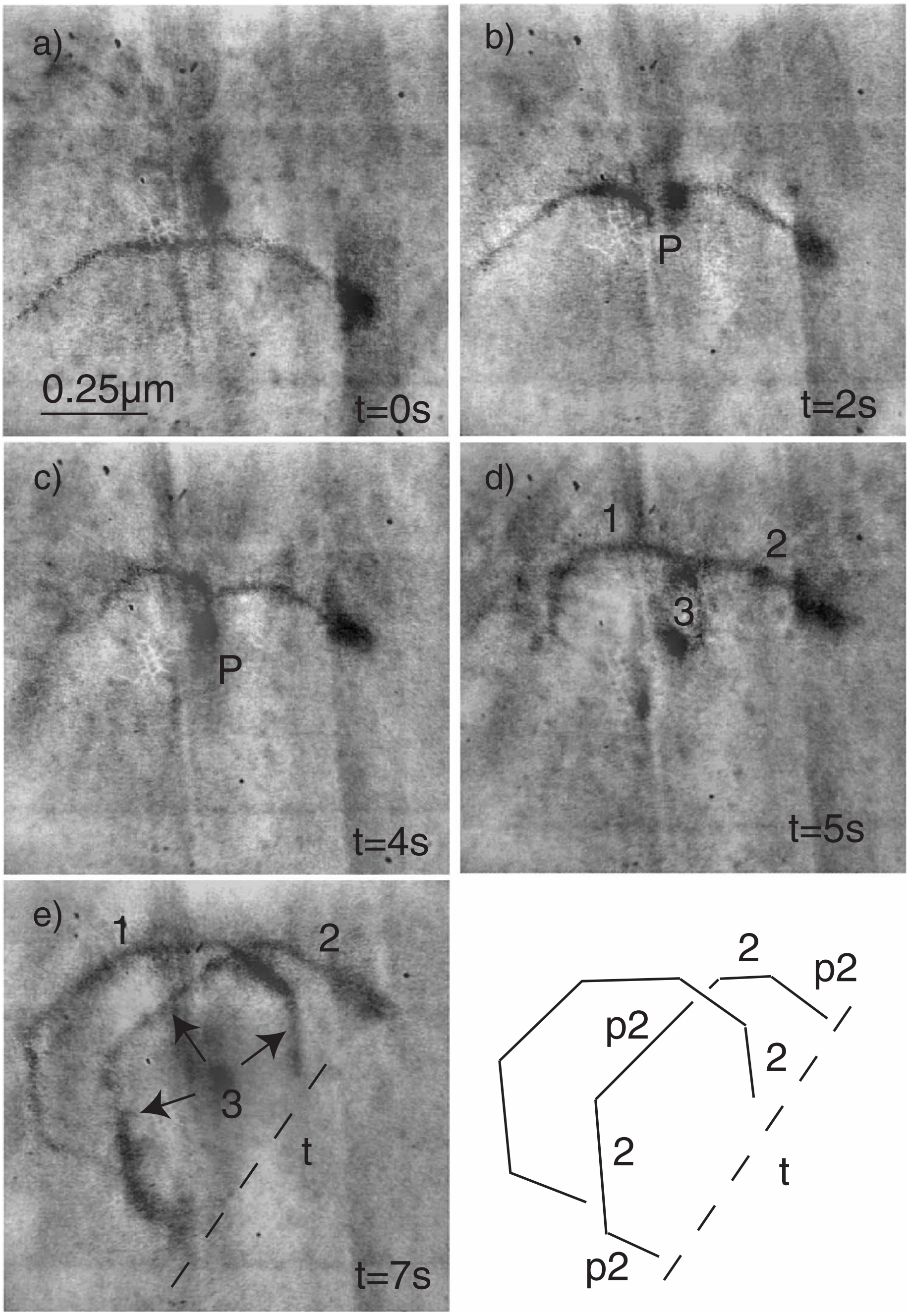

Figure 3. Dislocation multiplication at an open loop in a twofold plane at 720°C. P is a pinning point. Note the straight edges along twofold and pseudo-twofold directions.

twofold and pseudo-twofold directions, although the latter directions are less frequently observed than the former and, secondly, that the lateral motion of macrojogs can be much faster than the motion of straight segments (about 15 times in the example shown in figure 7).

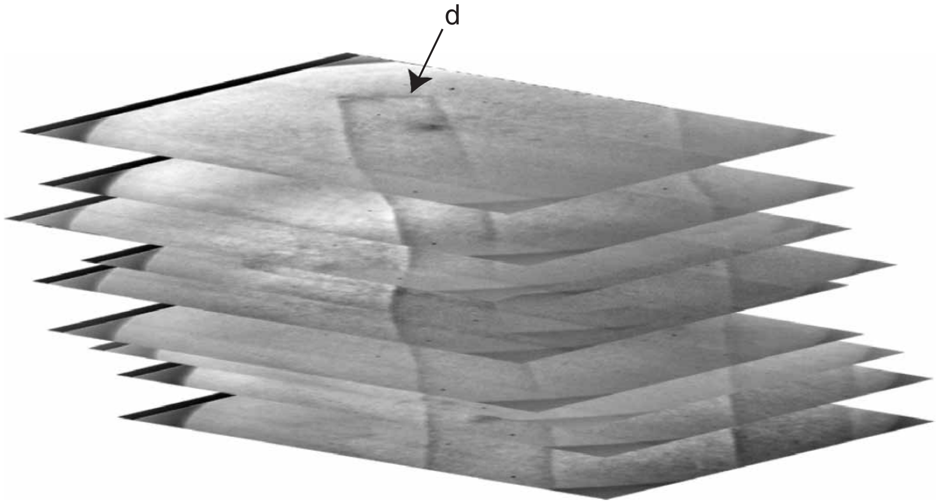

Figure 4. Wavy traces trailed by a dislocation d moving in a twofold plane, seen at a grazing angle.

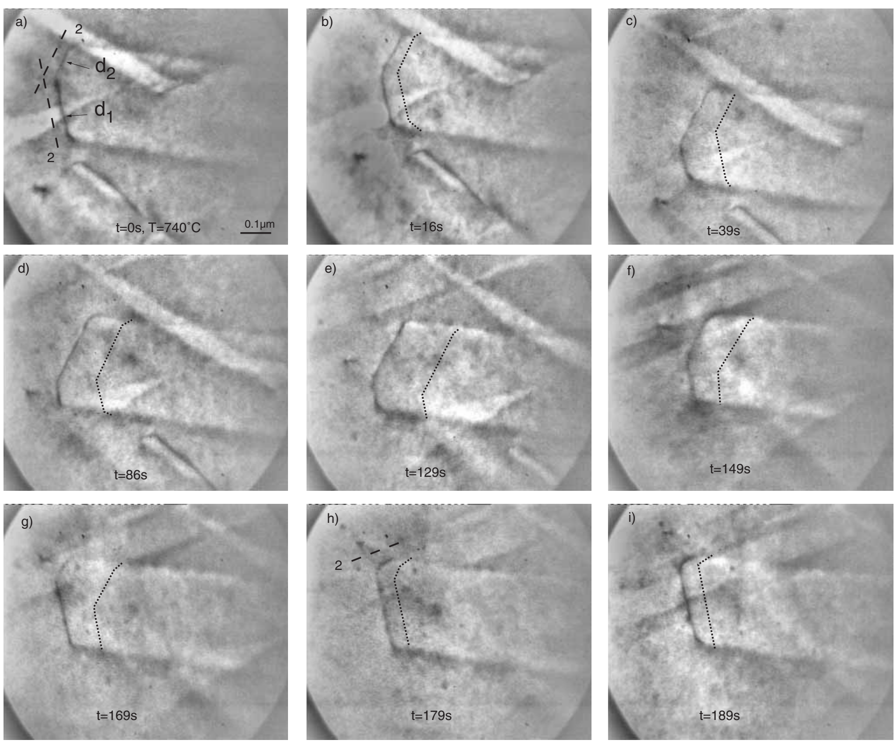

Figure 5. Dislocation motion in a fivefold plane, at 740°C. The dotted lines indicate the dislocation position in the previous frame. Note the straight edges parallel to twofold directions.

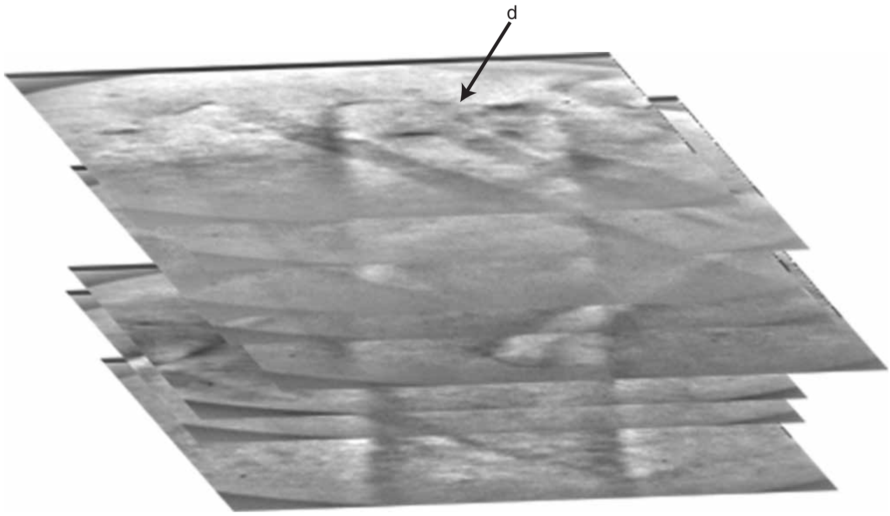

Figure 6. Straight traces left by a dislocation d moving in a fivefold plane, seen at a grazing angle.

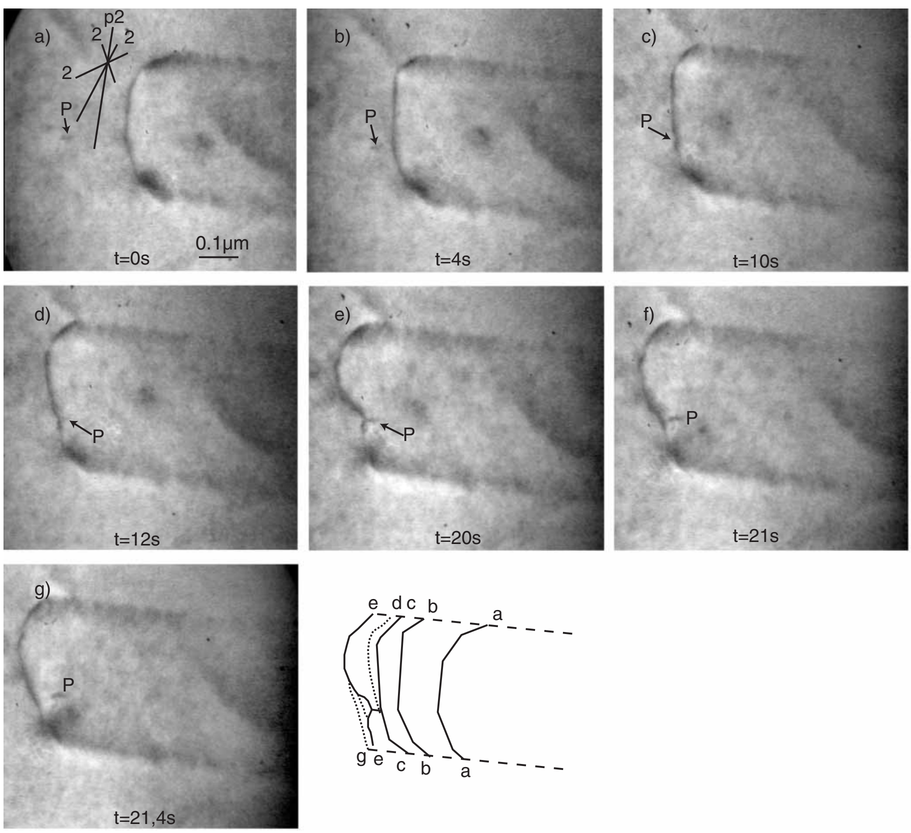

Figure 7. Dislocation motion in a fivefold plane (same as figure 5). Note the segment parallel to a pseudo-twofold direction in (a), the pinning at an extrinsic obstacle P and the fast motion of the macrojog after unpinning in (e)–(g).

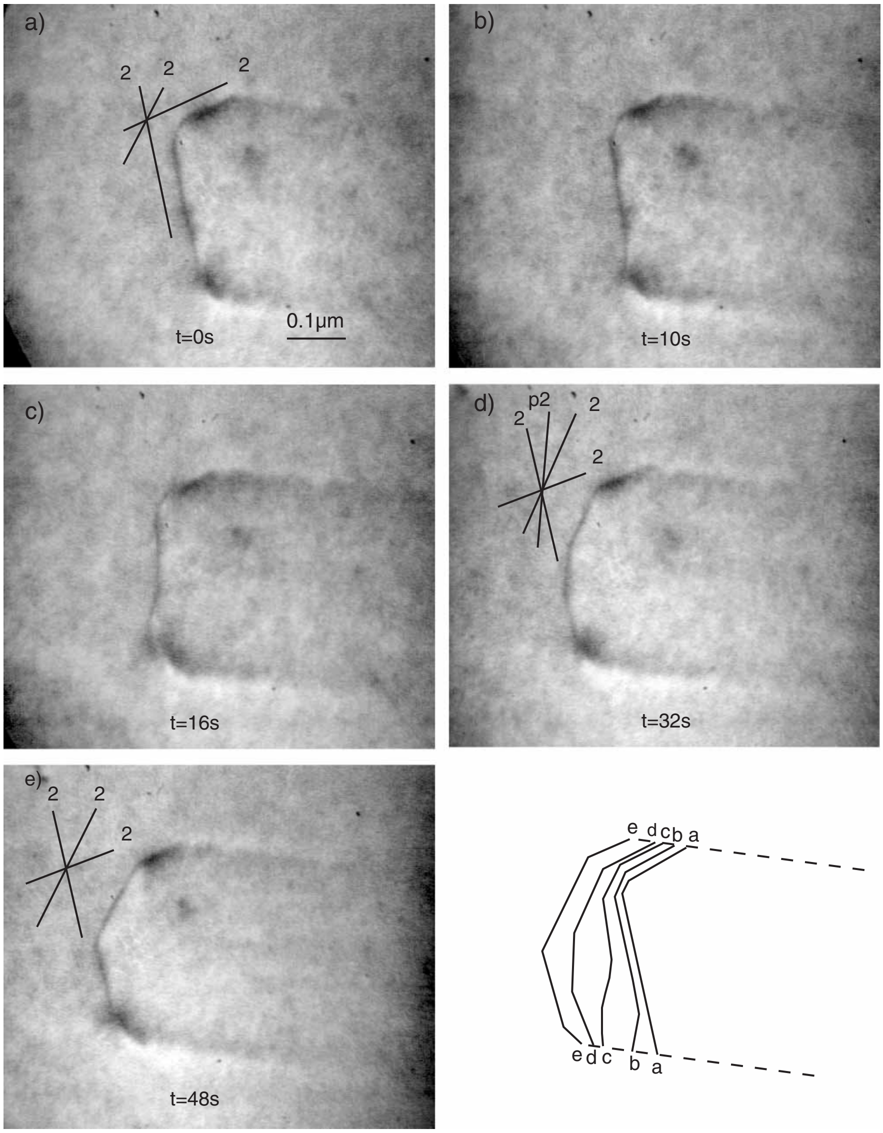

Figure 8. Dislocation motion in a fivefold plane (same as figures 5 and 7). Note the easy macrojog nucleation at a surface in (b) and (c), and the segment parallel to a pseudo-twofold direction in (d).

Figure 8 is the illustration of a dislocation behaviour frequently observed at free surfaces in thin foils. The dislocation shown in figure 7 moves steadily in a later stage of the experiment, with two segments parallel to twofold directions (figure 8 (a)). Then, the lower dislocation extremity accelerates, which results in the formation of a macrojog at the corresponding sample surface (figure 8 (b)). The macrojog moves rapidly along the dislocation (figures 8 (b) and (c)) and the dislocation recovers a polygonal shape with one segment along a pseudo-twofold direction (figure 8 (d)). This direction, however, seems to be less stable since only twofold edges remain after

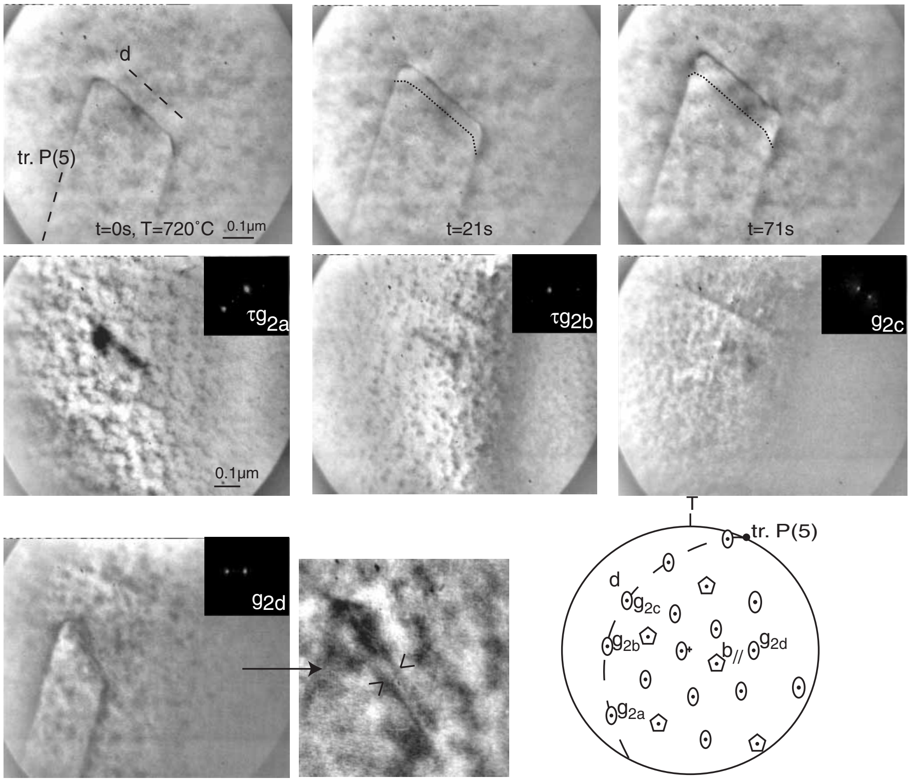

Figure 9. Dislocation motion in a fivefold plane, at 720°C and contrast analysis (see text).

further motion (figure 8 (e)). This again shows that pseudo-twofold directions are less stable than twofold directions in fivefold planes.

Figure 9 shows another dislocation moving in another fivefold plane. Its trace is denoted tr (P_5) in the stereographic projection. The dislocation lies along the direction d which is a twofold direction. It is out of contrast with diffraction vectors $\mathbf{g}_{2a}$ and $\tau\mathbf{g}_{2a}$ (with a strong residual contrast), $\mathbf{g}_{2b}$ and $\tau\mathbf{g}_{2b}$, $\mathbf{g}_{2c}$ and $\tau\mathbf{g}_{2c}$, all contained in the plane of motion. The Burgers vector is accordingly parallel to the fivefold direction perpendicular to the plane of motion. Since in addition a double contrast is observed with $\mathbf{g}_{2d}$, the Burgers vector could be fully determined as $A_0[\bar{1}1111\bar{1}]$, in the six-dimensional space ($A_0 = 0.645$ nm is the hyperlattice constant (Boudard *et al.* 1992)), with a component $\mathbf{b}_{//} = a_0\ [\bar{2}/2, 2/0, 0/0]$ (with $a_0 = A_0/[2(2+\tau)]^{1/2}$ (Cahn *et al.* 1986)) of length 0.563 nm in physical space (table 1).

3.3. *Dislocation motion in threefold planes and Burgers vector analysis*

Two dislocations moving in closely neighbouring parallel threefold planes, near the twofold sample plane, are shown in figure 10. They exhibit straight segments along twofold directions at an angle of 120°. They locally interact to form a short dipole that subsequently annihilates. Then, the acute angle between the two newly connected segments smooths rapidly (figure 10 (b)).

Another pair of dislocations moving in parallel threefold (1/1, 1/1, 1/1) planes is shown in figures 11 (a) and (b), in a fivefold sample heated at 700°C. They exhibit

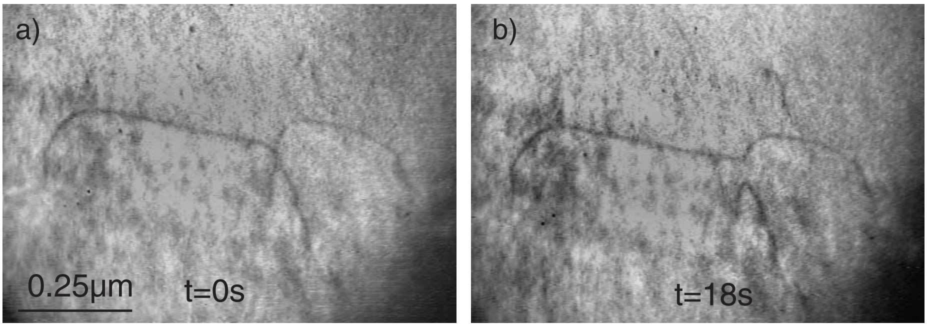

Figure 10. Dipole formation and annihilation on two dislocations moving in a threefold plane, at 740°C.

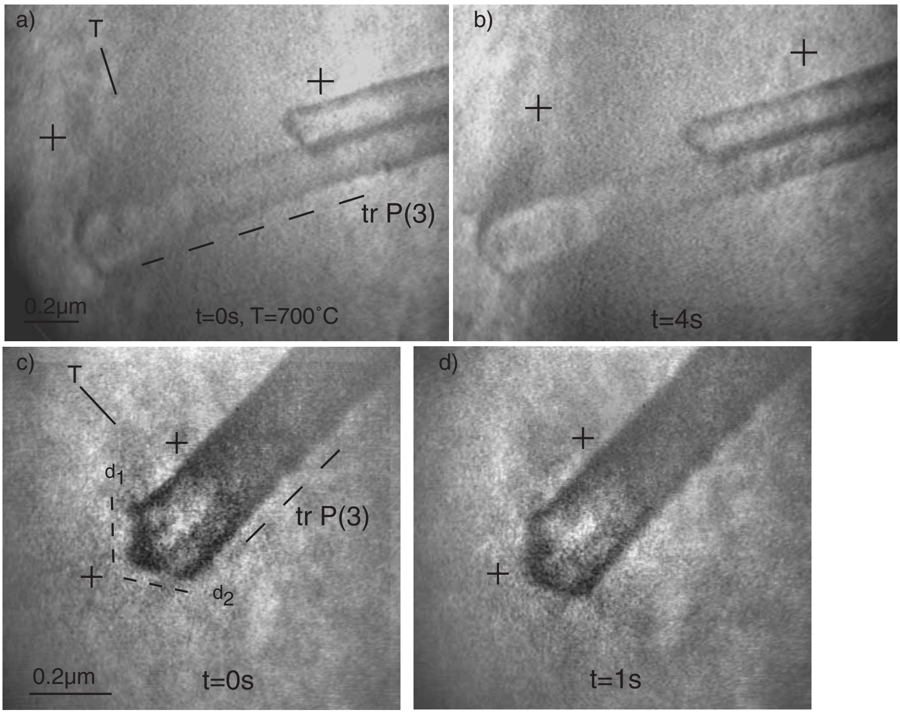

Figure 11. Dislocation motion in a threefold plane, at 700°C. Crosses indicate fixed points in the sample. Straight edges along twofold directions are seen.

two straight segments along twofold directions d_1 and d_2 at an angle of 120° (see enlargement in figures 11 (c) and (d)). These dislocations have been subsequently frozen by cooling the sample to room temperature, and their contrast has been studied under various diffraction conditions (see figure 12 and table 2). The main results of this contrast analysis are as follows.

(i) A strong extinction is found for $\mathbf{g}_{2d}$ and $\tau\mathbf{g}_{2d}$, as well as for $\mathbf{g}_{2e}$ and $\tau\mathbf{g}_{2e}$. The traces are out of contrast under the same conditions (figures 12 (g), (h), (j) and (k)).

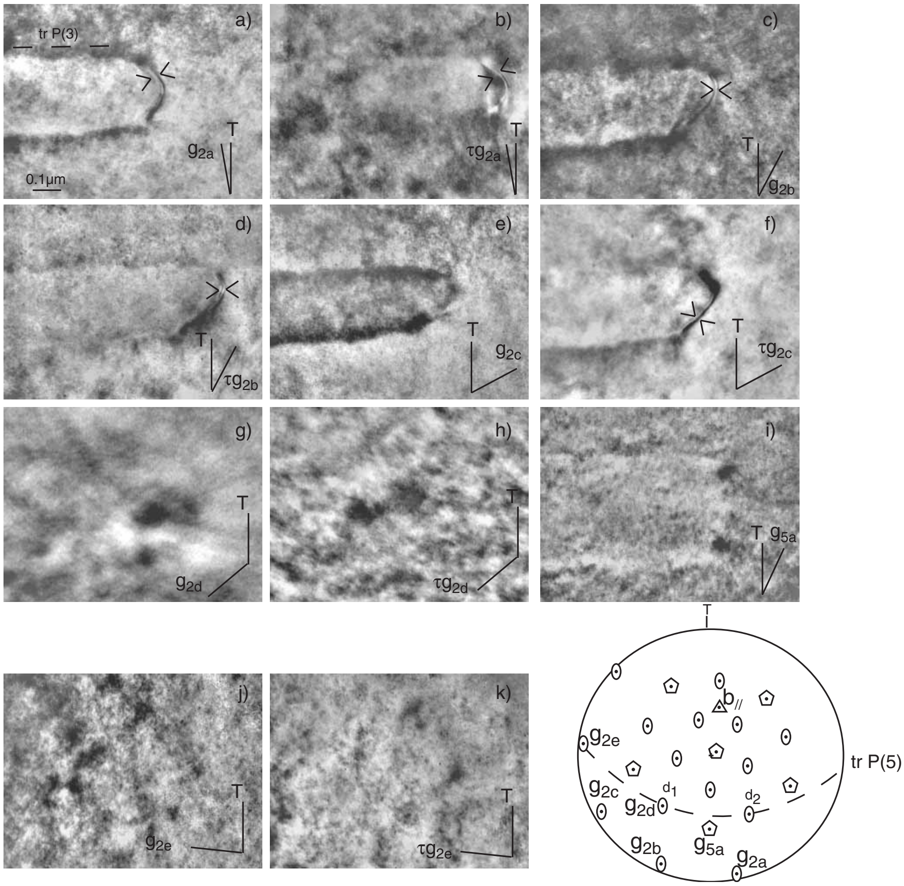

Figure 12. Contrast analysis of the dislocations in figure 11 (see text).

(ii) A double contrast is found for $\mathbf{g}_{2a}$ and $\tau\mathbf{g}_{2a}$, as well as for $\mathbf{g}_{2b}$ and $\tau\mathbf{g}_{2b}$ (figures 12 (a)–(d)).

(iii) A weak extinction is found for $\mathbf{g}_{2c}$ (with a faint broad residual contrast, in figure 12 (e)), and a double contrast for $\tau\mathbf{g}_{2c}$ (figure 12 (f)). The traces are not subjected to the weak extinction for $\mathbf{g}_{2c}$.

The strong extinctions show that the component of the Burgers vector in physical space is perpendicular to $\mathbf{g}_{2d}$ and $\mathbf{g}_{2e}$, that is perpendicular to the (1/1, 1/1, 1/1) plane of motion, which is perpendicular to a threefold direction. The observation of a weak extinction indicates that the quasicrystal is perfectly retiled around the dislocation; that is, its Burgers vector is a translation vector of the six-dimensional lattice. Exploiting the observation of the weak extinction and the double contrasts yield additional information that allows one to determine unambiguously the full Burgers vector. It can be determined as $\mathbf{B} = A_0[0\,0\,0\,\bar{2}\,2\,2]$ in six-dimensional space, possessing a physical space component $\mathbf{b}_{//} = a_0[\bar{2}/2, \bar{2}/2, \bar{2}/2]$ of 0.513 nm length (see table 2). Note that the vanishing contrast for the fivefold diffraction vector $\mathbf{g}_{5a}$ corresponds to a weak extinction ($\mathbf{g}_{5a}$ is indeed not perpendicular to $\mathbf{b}_{//}$). Traces are subjected to the same strong extinctions as dislocations because their strain fields in physical space

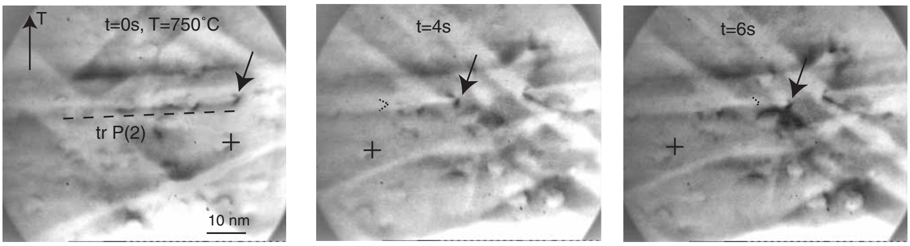

Figure 13. Dislocation motion in a specimen strained along the direction T, at 750°C. The dislocation (arrow) moves in an edge-on twofold plane (trace tr P(2)) perpendicular to the straining direction. The crosses indicates a fixed point.

are parallel. They are, however, not subject to the same weak extinctions because the corresponding amounts of retiling, that is the corresponding perpendicular-space strain fields, are generally different.

3.4. *Dislocation motion under uniaxial stress*

In-situ straining experiments were carried out on twofold samples with a twofold tensile axis T. The general behaviour of the dislocation motion closely resembles that observed upon mere heating. The planes of motion, however, are now related to the tensile axis. We most frequently find normals to these planes making angles of less than 54° with respect to the straining axis. Of particular interest is the observation of dislocations moving in the edge-on twofold plane perpendicular to the straining axis (figure 13). Such motion can be activated only by pure climb, because the corresponding orientation factor has its maximum possible value (equal to unity in pure climb) whereas it would be zero for pure glide (Mompiou *et al.* 2003). This conclusion can de derived because many *in-situ* observations show that the primary stress direction is locally parallel to the external stress direction in areas where deformation starts (Couret *et al.* 1993).

§4. Discussion

In this paper we report, for the first time, *in-situ* experiments including a direct analysis of dislocation motion and a full Burgers vector characterization of the same dislocations in a quasicrystalline material. The central result of these unique experiments is the provision of unambiguous evidence that dislocation motion in icosahedral Al–Pd–Mn takes place by pure climb. The results are in full agreement with indirect evidence previously obtained in post-mortem observations on as-grown specimens (Caillard *et al.* 1999, 2000, 2002a, b), and specimens deformed at low temperature (Mompiou *et al.* 2003). Our conclusions are drawn from the independent determination of planes of movement and Burgers vectors of single dislocations, the actual motion of which has been observed and recorded. Our conclusions are corroborated by further *in-situ* observations of dislocations moving in planes perpendicular to the direction of the tensile axis, for which the orientation factor is nil for glide, but maximum for climb. All models proposed so far, which postulated a glide motion, should thus be revised. Climb may be enhanced in thin foils owing to an easier nucleation or elimination of vacancies at the surfaces. However, evidence of the same climb mechanism in both as-grown and low-temperature compressed bulk specimens ensures the validity of the *in-situ* experiments.

Climb motions in twofold, threefold and fivefold planes take place at comparable velocities. Climb is wavier in twofold planes than in fivefold planes, in agreement with results of post-mortem observations in as-grown samples by Caillard *et al.* (2000, 2002a). The wavy climb motion in twofold planes favours extensive dislocation multiplication via open loops (figure 3), which accounts for the bundles of twofold dislocations moving in closely neighbouring parallel twofold planes, observed previously in as-grown samples (Caillard *et al.* 2000). Other sites of dislocation multiplication are thought to be Bardeen–Herring sources. Easy dislocation multiplication leads to the strong yield drop observed at the onset of plastic deformation (Feuerbacher *et al.* 1997). Conversely, since dislocation annihilation is easier when climb is allowed (figure 10), the decrease in dislocation density observed at increasing strain is also satisfactorily explained (Schall *et al.* 1999).

Two types of motion are observed as a function of temperature and dislocation velocity. At a given temperature, and in a given area, fast dislocations trail a rapidly vanishing phason fault, whereas no fault can be seen in the wake of the slowest dislocations. If t is the lifetime of phason faults before dissolution, the length λ of the fault trailed by a dislocation moving at a velocity v is given by $\lambda = vt$; that is, it is shorter for slower dislocations. For the slowest dislocations, λ is too small to be detected. These dislocations can accordingly be considered as continuously perfect. The simultaneous observation of both types of motion at a given temperature shows that trailing a phason fault does not generally provide a sufficiently high frictional force to inhibit fast dislocation motion. This result is consistent with the low values of phason-fault energies, estimated from dissociation-width measurements. These values indeed correspond to a back stresses substantially lower than the flow stress. While back-stress values of about 30 MPa are found (Mompiou *et al.* 2003), typical flow-stress values are of the order of 500 MPa at 700°C (Feuerbacher *et al.* 1997).

Mobile dislocations exhibit straight segments along twofold directions in twofold, threefold and fivefold planes, and along pseudo-twofold directions in twofold planes and, to a less extent, in fivefold planes (threefold planes do not contain pseudo-twofold directions). Accordingly, dislocations in twofold planes have pseudo-octagonal shapes (with angles of 122° and 148°; see figure 3), whereas those in fivefold planes generally remain decagonally shaped (see figure 5 and see also figures 2 and 3 of the paper by Caillard *et al.* (2002b)). This shows that the dislocation line energy is strongly orientation dependent.

It is worth noting that this property could be verified for all Burgers vectors and planes of motion: threefold dislocations in threefold planes (figures 10 and 11), fivefold dislocations in fivefold planes (figures 5, 7 and 8) and twofold dislocations in fivefold planes (Caillard *et al.* 2002a). We have furthermore indirect evidence for twofold dislocations in twofold planes (see figure 3), for which, however, undoubted Burgers vector determinations still have to be carried out. The origin of a lower dislocation-core energy along twofold and pseudo-twofold directions is unknown. Since the elastic properties of icosahedral Al–Pd–Mn are fairly isotropic (Amazit *et al.* 1992), this dependence is more probably related to a nonplanar extended core configuration, as found for screw dislocations in bcc metals, or to covalent bonding, as found in semiconductors. Takeuchi *et al.* (2002) estimated the dislocation core energy as a function of its displacement and found minima corresponding to a quasiperiodic Peierls potential. Although this rough estimation was aimed at the understanding of frictional forces for glide motion, it may be transposed to the case of climb.

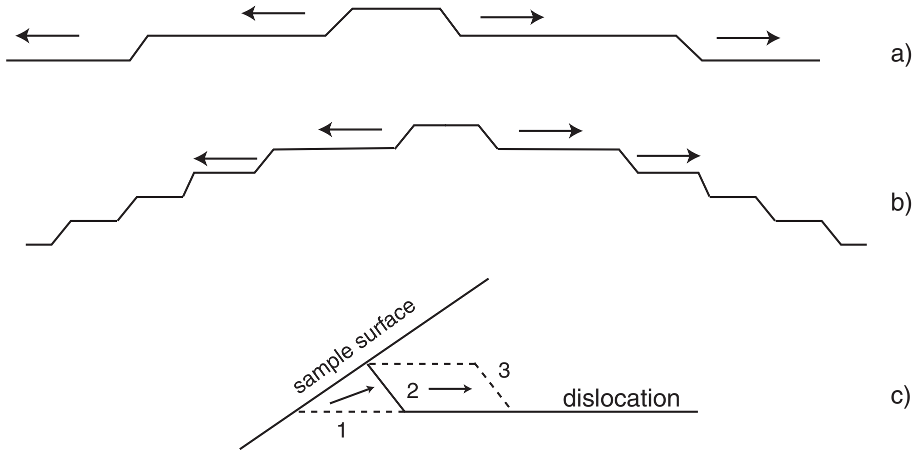

Figure 14. Schematic diagrams of (a) slow jog-pair nucleation and fast jog propagation, yielding a straight moving dislocation, (b) fast jog-pair nucleation and slow jog propagation, yielding a curved moving dislocation, and (c) easy jog nucleation at a free surface.

The rectilinear aspect of moving dislocations also shows that climb takes place by the nucleation of jog pairs at low rates, followed by rapid climb of the jogs along the dislocation line. According to figure 14, moving dislocation segments remain rectilinear only if the density of moving jogs is low, namely if the time for nucleating jog pairs is smaller or of the order of the time necessary to move them to dislocation extremities. Conversely, a slow jog motion and a high jog-pair nucleation rate would lead to curved moving dislocations (figure 14 (b)). This conclusion is in agreement with the fairly fast motion of macrojogs compared with the rather slow motion of rectilinear segments observed in figure 7. A similar type of climb motion, controlled by low-rate nucleation of jog pairs, was also observed for the growth of vacancy loops in quenched and annealed metals (Smallman and Westmacott 1972). The enhanced jog nucleation observed at the sample surface, as seen in figure 8, can be attributed to a gain of dislocation line energy during its formation, as shown in figure 14 (c).

§ 4. Conclusions

In-situ observations of dislocation motion in icosahedral Al–Pd–Mn quasicrystals have yielded the following results.

(1) Dislocations with twofold, threefold and fivefold Burgers vectors move by pure climb in twofold, threefold and fivefold planes respectively. No indication for glide motion has been observed for more than ten fully investigated *in-situ* dislocation movements.
(2) Dislocation motion is rather planar in threefold and fivefold planes, and significantly wavier close to twofold planes.
(3) Dislocations multiply and annihilate by climb.
(4) Moving dislocations with twofold, threefold and fivefold Burgers vectors exhibit straight line segments parallel to twofold directions and (in twofold planes and to a less extent in fivefold planes) pseudo-twofold directions. This

and the observation of fast macrojog motion show that climb involves a low-rate jog-pair nucleation and an easier jog climb motion along the dislocation line.

(5) At 700°C, fast dislocations are partials trailing a rapidly dissolving phason fault whereas slow dislocations are perfect. Their simultaneous occurrence shows that the back force due to trailed phason faults is much weaker than the driving force for climb.

Acknowledgements

M. F. is indebted to the Ministère de la Jeunesse, de l'Education Nationale et de la Recherche, for a senior scientist fellowship grant to pursue part of his research in Toulouse.

References

Amazit, Y., de Boissieu, M., and Zarembowitch, A., 1992, *Europhys. Lett.*, **20**, 703.

Boudard, M., De Boissieu, M., Janot, Ch., Heger, G., Beeli, C., Nissen, H. U., Vincent, H., Ibberson, R., Audier, M., and Dubois, J. M., 1992, *J. Phys: condens. Mater*, **50**, 10 149.

Cahn, J. W., Shechtman, D., and Gratias, D., 1986, *J. Mater. Res.*, **1**, 13.

Caillard, D., 2000, *Quasicrystals, Current Topics*, edited by E. Belin-Ferré, C. Berger, M. Quiquandon and A. Sadoc (Singapore: World Scientific), p. 387.

Caillard, D., Mompiou, F., Bresson, L., and Gratias, D., 2003, *Scripta mater.*, **49**, 11.

Caillard, D., Mornirolli, J. P., Vanderschaeve, G., Bresson, L., and Gratias, D., 2002a, *Eur. Phys. J., appl. Phys.*, **20**, 3.

Caillard, D., Roucau, C., Bresson, L., and Gratias, D., 2002b, *Acta mater.*, **50**, 4499.

Caillard, D., Vanderschaeve, G., Bresson, L., and Gratias, D., 1999, *Mater. Res. Soc. Symp. Proc.*, **553**, 301; 2000, *Phil. Mag.* A, **80**, 237.

Couret, A., and Caillard, D., 1985, *Acta metall.*, **33**, 1447.

Couret, A., Crestou, J., Farenc, S., Molénat, G., Clément, N., Coujou, A., and Caillard, D., 1993, *Microsc. Microanal. Microstruct.*, **4**, 153.

Feuerbacher, M., Metzmacher, C., Wollgarten, M., Baufeld, B., Bartsch, M., Messerschmidt, U., and Urban, K., 1997, *Mater. Sci. Engng*, **A233**, 133.

Feuerbacher, M., Mompiou, F., and Caillard, D., 2004 (to be published).

Messerschmidt, U., Bartsch, M., Feuerbacher, M., Geyer, B., and Urban, K., 1999, *Phil. Mag.* A, **79**, 2123.

Messerschmidt, U., and Bartsch, M., 2003, *Scripta mater.*, **49**, 33.

Mompiou, F., Bresson, L., Cordier, P., and Caillard, D., 2003, *Phil. Mag.*, **83**, 3133.

Rosenfeld, R., Feuerbacher, M., Baufeld, B., Bartsch, M., Wollgarten, M., Hanke, G., Beyss, M., Messerschmidt, U., and Urban, K., 1995, *Phil. Mag. Lett.*, **72**, 375.

Schaaf, G. D., Mikulla, R., Roth, J., and Trebin, H. R., 2000, *Mater. Sci. Engng*, **A294–296**, 799.

Schall, P., Feuerbacher, M., Messerschmidt, U., and Urban, K., *Phil. Mag. Lett.*, **79**, 1999.

Smallman, R. E., and Westmacott, K. H., 1972, *Mater. Sci. Engng.*, **9**, 249.

Takeuchi, S., Tamura, R., Kabutova, E., and Edagawa, K., 2002, *Phil. Mag.* A, **82**, 379.

Wollgarten, M., Bartsch, M., Messerschmidt, U., Feuerbacher, M., Rosenfeld, R., Beyss, M., and Urban, K., 1995, *Phil. Mag. Lett.*, **71**, 99.

Wollgarten, M., Beyss, M., Urban, K., Liebertz, H., and Kocster, U., 1993, *Phys. Rev. Lett.*, **71**, 543.

Wollgarten, M., Gratias, D., Zhang, Z., and Urban, K., 1991, *Phil. Mag.*, **64**, 819.

Yang, W., Feuerbacher, M., Tamura, N., Ding, D., Wang, R., and Urban, K., 1998, *Phil. Mag.* A, **77**, 1481.